View metadata, citation and similar papers at core.ac.uk
brought to you by CORE
provided by NASA Technical Reports Server

Large-eddy simulation of flow past a circular cylinder

By R. Mittal

1. Motivation and objectives

Some of the most challenging applications of large-eddy simulation are those in complex geometries where spectral methods are of limited use. For such applications more conventional methods such as finite difference or finite element have to be used. However, it has become clear in recent years that dissipative numerical schemes which are routinely used in viscous flow simulations are not good candidates for use in LES of turbulent flows. Except in cases where the flow is extremely well resolved, it has been found that upwind schemes tend to damp out a significant portion of the small scales that can be resolved on the grid. Furthermore, it has been found that even specially designed higher-order upwind schemes that have been used successfully in the direct numerical simulation of turbulent flows produce too much dissipation when used in conjunction with large-eddy simulation.

A case in point is the LES of flow past a circular cylinder performed by Beaudan & Moin (1994) at a Reynolds number of 3900. One of the objectives of this investigation was to study the suitability of higher order upwind-biased schemes for LES of complex flows and to validate the methodology against experimental results of Ong & Wallace (1994) and Lourenco & Shih (1993). In particular, 5^{th}- and 7^{th}-order schemes were used for these simulations. The 5^{th}-order scheme has been successfully used for DNS of transition and turbulence in flow over a flat plate by Rai & Moin (1993) and it was thought that these schemes would be useful in LES of flows in complex geometries. However, the conclusion of the study by Beaudan & Moin (1994) was that except in regions where the mesh was fine enough to resolve a significant portion of the small scales, numerical dissipation overwhelmed the contributions from the subgrid-scale eddy-viscosity model.

In contrast to upwind-biased schemes which control aliasing through numerical dissipation, aliasing is controlled in central schemes by an energy conservation principle. Such schemes do not exhibit numerical dissipation and, therefore, there is no spurious damping of the smaller scales. This feature makes the schemes attractive for use in LES of complex flows. The downside of using such schemes is the dominance of dispersive error, which makes these schemes extremely sensitive to aspects such as the grid stretching factors (Cain & Bush, 1994) and outflow boundary conditions (Gresho & Lee 1981). Thus, even though the central schemes might have a clear advantage over upwind biased schemes in simple geometries, in more complex geometries where complicated grids are used, the superiority of central schemes needs to be established and this is the motivation of the current study.

The objective of the current study is to perform a LES of incompressible flow past a circular cylinder at a Reynolds number of 3900 using a solver which employs an

energy- conservative second-order central difference scheme for spatial discretization and compare the results obtained with those of Beaudan & Moin (1994) and with the experiments in order to assess the performance of the central scheme for this relatively complex geometry.

Salient features of the simulation of Beaudan & Moin (1994):

Beaudan & Moin (1994), henceforth refered to as BM, simulated the flow past a circular cylinder on an O-mesh using a compressible flow solver. One point upwind-biased 5^{th}- and 7^{th}-order schemes were used for the spatial discretization of the convective terms. The simulations were carried out on a $144\times136\times48$ ($r\times\theta\times z$) grid and good resolution was provided near the cylinder surface and in the near wake region ($x/D < 2.0$). Beyond this region, the grid was stretched geometrically in the streamwise direction such that the streamwise grid spacing at $x/D = 10.0$ was about $0.13D$. The mesh near the outflow boundary was made extremely coarse in order to damp out disturbances and a convective outflow boundary condition was used. Grid stretching ratios in excess of 10% were used to obtain the desired grid spacing in the wake.

Simulations were carried out with no subgrid-scale model, with a fixed coefficient Smagorinsky model and with the spanwise averaged version of the dynamic model (Ghosal *et al.*, 1995, Moin *et al.* 1991). It was observed that mean wall statistics such as drag, pressure coefficients, wall shear stress and separation angles were not significantly different in the three simulations and all showed reasonable agreement with experimental data. In the vortex formation region ($x/D < 4.0$), it was found that the dynamic model predicted mean velocities and Reynolds stresses which were in better agreement with the experimental results than the other two simulations. Beyond this region the difference between the three computed solutions diminished such that the solutions were virtually indistinguishable beyond $x/D > 7.0$. It was found that in this region where the mesh was relatively coarse, numerical dissipation overwhelmed the contribution of the SGS model. The simulation with the 7^{th}-order scheme showed evidence of increased energy in the high wavenumbers, but here too it was found that a substantial portion of the resolvable wavenumber range was damped due to numerical dissipation. It was concluded that these high order upwind-biased schemes were unsuitable for use in LES.

2. Accomplishments

2.1 Numerical method

The solver used in the current work is based on the solver developed by Choi *et al.* (1992) and employs a second-order central-difference method written in generalized coordinates in a spanwise periodic domain. Velocity components and pressure are fully staggered in order to strictly conserve mass in the generalized coordinates. It should be pointed out that strict conservation of momentum and energy is not guaranteed on a non-equispaced mesh. The solution is advanced in time using a fractional step scheme wherein a third-order Runge-Kutta scheme and a Crank-Nicolson scheme is used for the nonlinear convection terms and viscous terms respectively. A multigrid solver is used in conjunction with a Gauss-Siedel line-zebra scheme

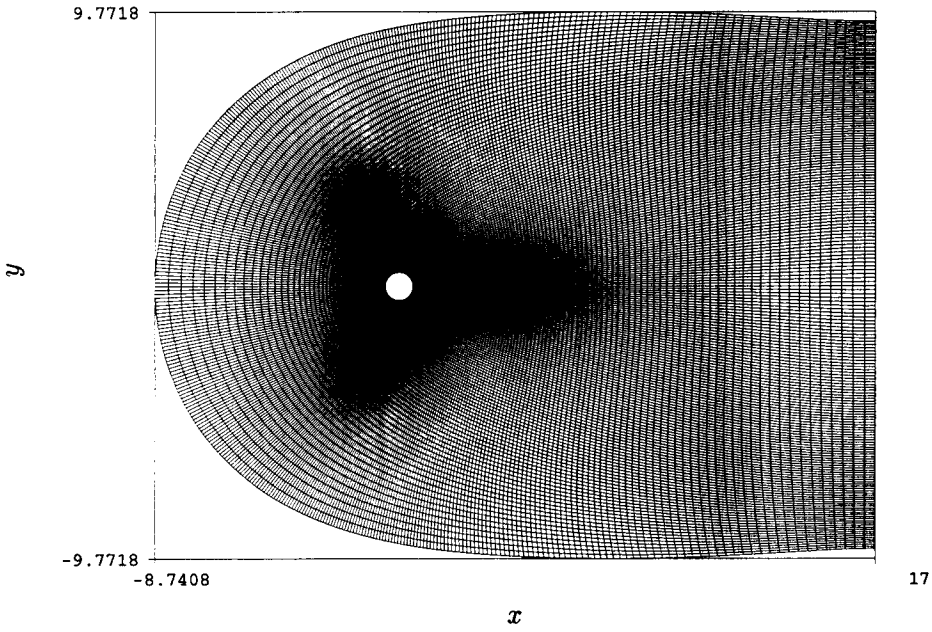

FIGURE 1. C-mesh used for Run-II.

for solving the pressure Poisson equation. The solver employs a spanwise-averaged version of the dynamic model where the total viscosity is constrained to be greater than zero (Ghosal *et al.*, 1995). The spanwise length of the cylinder is chosen to be πD which is the same as BM.

A C-mesh is used for the present simulations (Fig. 1). This type of mesh is ideally suited for simulating wake flows since better streamwise resolution can be selectively provided in the wake region. The use of a C-mesh also simplifies the application of outflow boundary conditions. Furthermore, another advantage of using a C-mesh is that as the flow separates from the cylinder, it remains roughly aligned with one family of grid lines, and thus good control over the streamwise stretching ratio can be maintained in this region. It has been found that in LES, where the resolution is at best marginal, central schemes can tolerate only a small streamwise stretching factor ($< 3\%$). Higher stretching factors can leads to the amplification of grid-to-grid oscillations ($2-\Delta$ waves). If an O-type mesh were to be used for the present simulations, the flow in the region of the separated shear layer would experience large strething ratios as it would go from being aligned with one family of grid lines to being aligned with the other, and solution in this region would be contaminated by $2-\Delta$ waves. Thus, the use of a C-mesh is necessary for obtaining a good solution with the current solver. This brings in the important point that the grid has to be designed keeping in mind the underlying spatial discretization.

2.2 Simulation results and discussion

The first simulation (Run I) was carried out on a 329×100×48 mesh with 80 points on the cylinder surface, 125 streamwise points along the wake centerline, 100 points in the wall normal direction, and 48 points along the spanwise direction. Since this was the first simulation, a relatively coarse mesh was chosen with the objective that results from this simulation would provide an estimate of the resolution requirements. The results from this simulation are summarized in Table 1. Also tabulated for direct comparison are the corresponding results from the 2-D simulation and 3-D LES of BM and experimental results from various studies. This simulation predicted a higher mean drag, rms lift, and base suction pressure coefficient than the corresponding LES of BM and experiments. Furthermore, it was observed that the computed in-plane Reynolds stresses ($\overline{u'^2}$, $\overline{v'^2}$ and $\overline{u'v'}$) in the near wake were significantly higher than the corresponding LES of BM and experiments of Lourenco & Shih (1993). On the other hand, spanwise Reynolds normal stress ($\overline{w'^2}$) in the near wake was under-predicted. All indications were that the flow was not developing enough three-dimensionality.

To get a realistic evolution of the three-dimensionality in the near wake, one requires adequate resolution of the underlying two-dimensional flow in addition to good spanwise resolution of the three-dimensional structures. It was clear that the azimuthal resolution of the attached boundary layer and separation region was much less than in the LES of BM. This could possibly lead to an incorrect location of the separation point and subsequent evolution of the separated shear layer. Therefore, it was decided to continue the simulation on a mesh with increased azimuthal resolution on the cylinder surface.

The second simulation (Run-II) was carried out on a 399×100×48 mesh where the number of points on the cylinder surface was increased from 80 to 150. In order to maintain a smooth streamwise distribution of grid points at the concave corner in the base of the cylinder, streamwise resolution had be improved marginally (by about 10%) in the near wake. The grid was kept roughly the same in all other regions. Some of the results of this simulation are summarized in Table 1. It was observed that overall there was no substantial improvement in the results. The mean drag coefficient, rms lift coefficient, and base pressure coefficient all show a small change towards the correct values but the results are still significantly different from BM and experiments.

In Fig. 2 is shown the variation of lift and drag coefficient with time after the flow has reached a statistically stationary state. All the data presented for this simulation has been averaged over the time period shown in this figure. Figure 3 shows the distribution of the surface pressure coefficient obtained from the present simulations. Results of BM have also been plotted for comparison. It is clear that the current simulations predict a significantly higher suction pressure in the wake region and that increasing the azimuthal resolution on the cylinder surface has only a marginal effect on the surface pressure distribution.

Figures 4a and 4b show the streamwise and cross-stream mean velocity profiles in the near wake ($x/D = 1.54$) obtained from the current simulations. Figure 4a

Table 1. Wall Statistics

	Run − I	*Run − II*	*Beaudan&Moin* (3 − *D*)	*Beaudan&Moin* (2 − *D*)	*Lourenco &Shih*
$\overline{C_{Pb}}$	−1.28	−1.15	−0.95	−2.16	−0.9±0.05
$\overline{C_D}$	1.2	1.1	1.0	1.74	0.98±0.05
$\overline{\theta_s}$	89°	88°	85.8°	108.1°	85°±2°

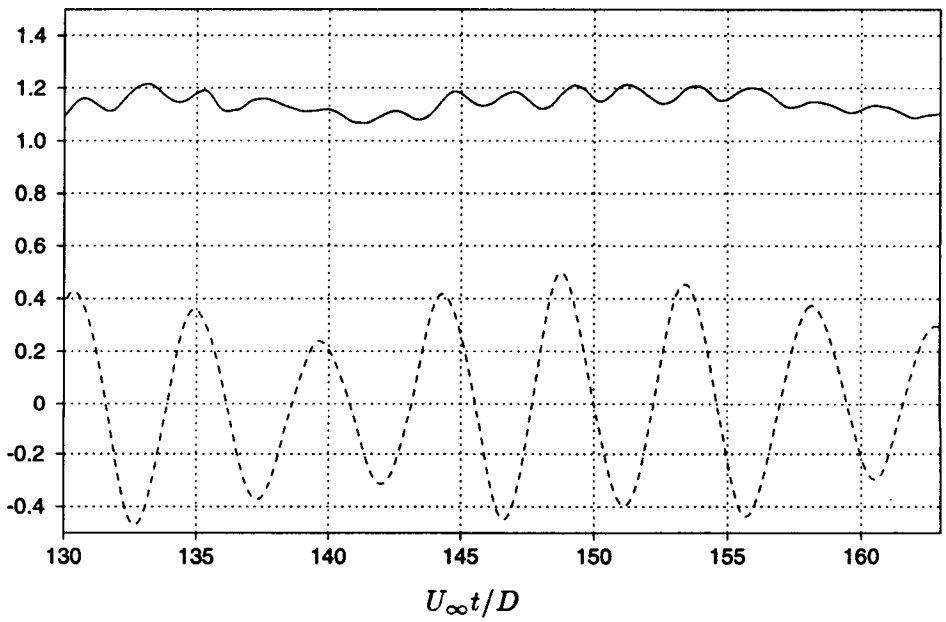

FIGURE 2. Variation of lift and drag coefficient with time obtained from Run-II. —— C_D; ---- C_L.

shows that the current simulations underpredict the momentum deficit in the near wake, and consequently the wake bubble length is also underpredicted (see Table 1). In contrast to the streamwise velocity, the mean cross-stream velocity (Fig. 4b) matches well with the results of BM. Furthermore, it is observed that the experimental data does not match with any of the simulation results. This is consistent with the fact that Beaudan & Moin (1994) indicated that large errors might be present in the experimental measurements (Lourenco & Shih, 1993) of cross-stream velocity in the near wake.

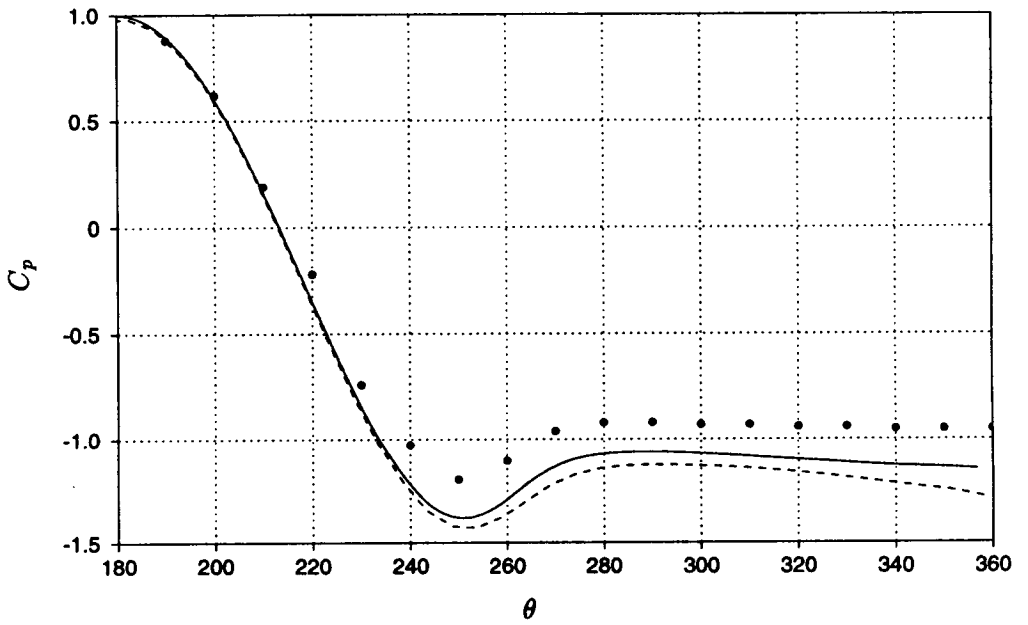

FIGURE 3. Variation of pressure coefficient on the surface of the cylinder. —— Run-II; ---- Run-I; • Beaudan & Moin.

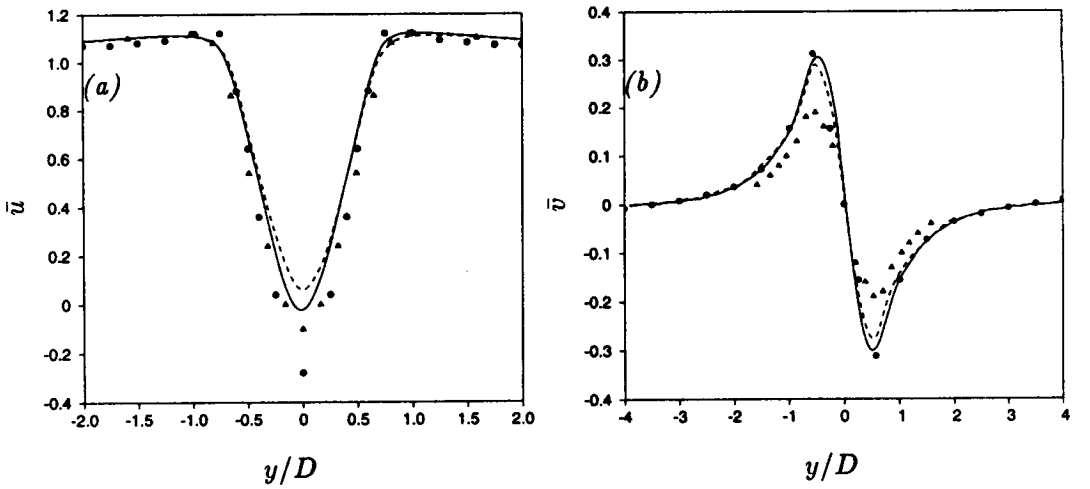

FIGURE 4. Mean velocity profiles at $x/D = 1.54$. (a) Streamwise velocity. (b) Cross-stream velocity. —— : Run-II; ---- : Run-I; • : Beaudan & Moin; ▲ : Lourenco & Shih.

In Fig. 5 are shown Reynolds stress profiles at this streamwise location. It can be observed from Fig. 5a that the current simulations over-predict the streamwise

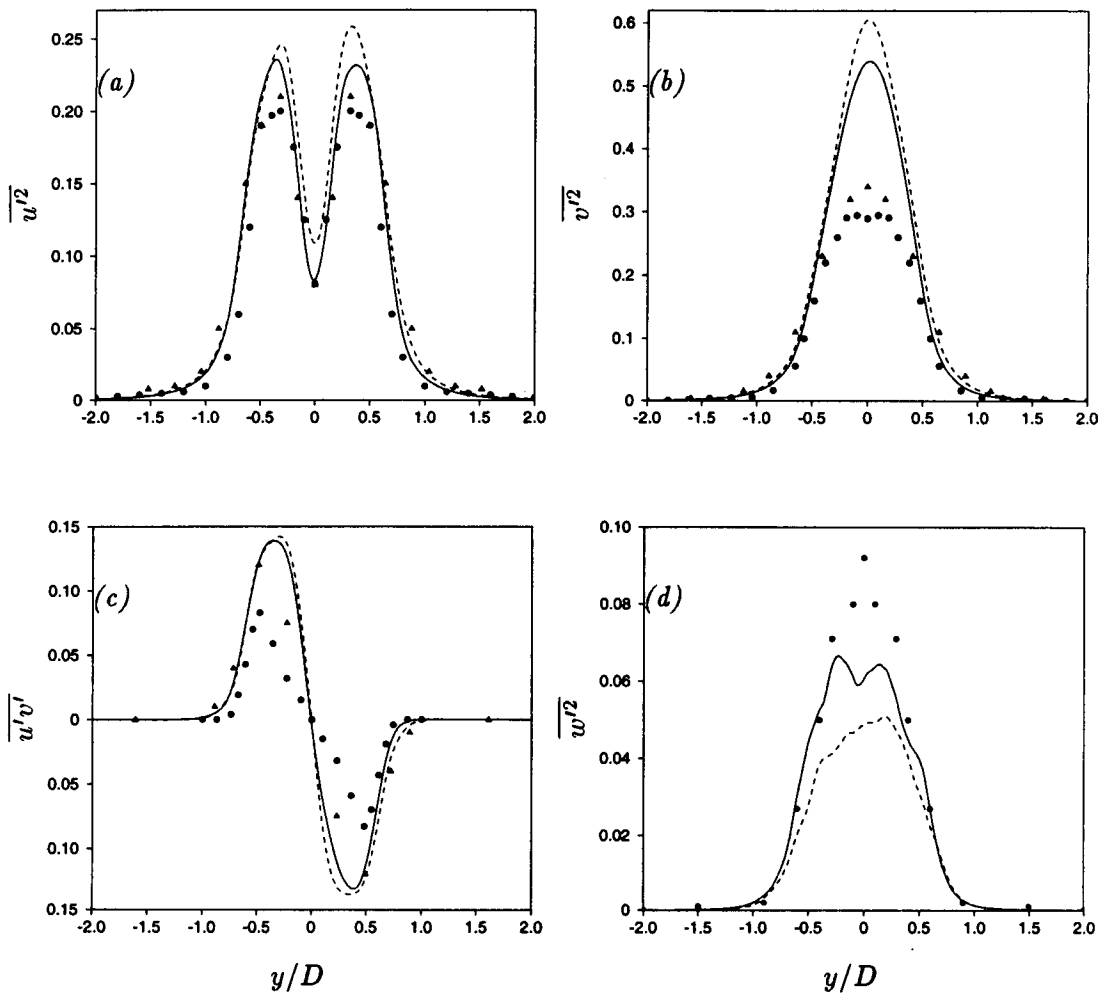

FIGURE 5. Reynolds stress profiles at $x/D = 1.54$. (a) $\overline{u'^2}$ (b) $\overline{v'^2}$ (c) $\overline{u'v'^2}$ (d) $\overline{w'^2}$ ——— : Run-II; ---- : Run-I; • : Beaudan & Moin; ▲ : Lourenco & Shih.

Reynolds stress ($\overline{u'^2}$). However, overall, the stress profile is better predicted in Run-II. The noticeable asymmetry of the profile about the wake ceneterline obtained from Run I also suggests that more than six shedding cycles might be needed for averaging the statistics. Figure 5b shows the corresponding profiles of cross-stream normal Reynolds stress ($\overline{v'^2}$), and here large differences between the results of the current simulations and the results of BM can be seen. Run-I and Run-II over-predict the peak stress by about 100% and 80% respectively. A similar trend is observed in Fig. 5c, in which profiles of ($\overline{u'v'}$) are plotted.

Figure 5d shows profiles of the spanwise Reynolds normal stress, and we observe that the current simulation under-predicts this stress component. There is however,

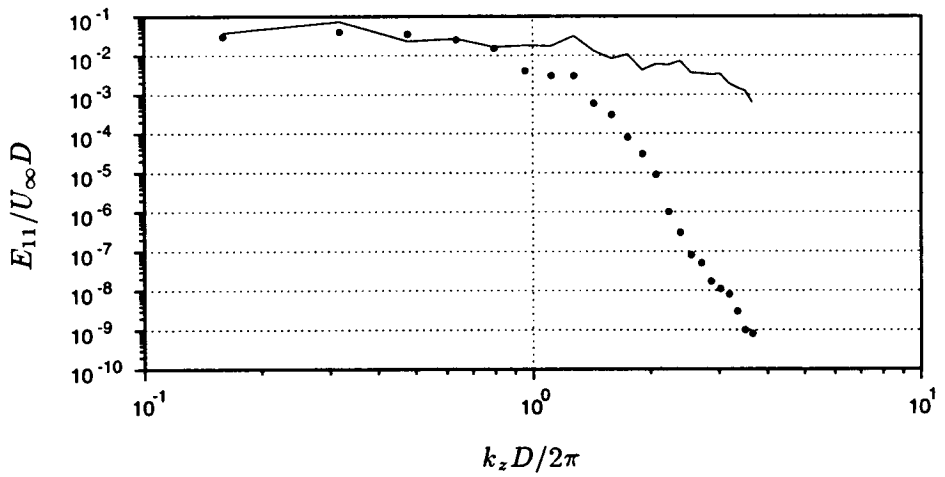

FIGURE 6. One-dimensional spectra at $x/D = 0.7$, $y = 0$. —— :Run-II; • : Beaudan & Moin.

a noticeable effect of increasing the azimuthal surface resolution on this stress component. First the peak stress obtained from Run-II is about 17% higher than that obtained from Run-I. A more noticeable effect is that in Run-II a 'fuller' profile is obtained in the region y/D>0.25 and this is in much better agreement with BM. This is most likely due to improved streamwise resolution in the near wake which leads to increase in the growth of three-dimensional instability in this region.

Figure 5 shows clear evidence that in the current simulations, the flow is not developing enough three-dimensionality in the near wake. As a result of this, in-plane stresses are over-predicted and spanwise stresses are under-predicted. It has been shown that the in-plane Reynolds stresses play a significant role in determining the base suction pressure (Mittal & Balachandar, 1995). Thus the higher in-plane Reynolds stresses lead to a higher base suction pressure and drag in the current simulations.

Figure 6 shows the spanwise one-dimensional spectra of the streamwise velocity in the near wake obtained from Run-II and the simulation of BM. Direct comparison of the spectra can be made since both simulations employ the same resolution in the spanwise direction. It can be observed that the two spectra match well only for the low wavenumbers (approximately 20% of the wavenumber range). Beyond this range, the spectra obtained by BM exhibits significant damping and the energy shows a decay of about seven orders of magnitude. In contrast, the spectra obtained from the current simulation is relatively flat with about one order of magnitude decay in the high wavenumber range. It should be pointed out that comparison of spanwise spectra at other wake locations shows a similar trend. Thus, it is clear that the higher-order upwind scheme used in the simulation of BM damps out a significant portion of the wavenumbers that can be resolved on the grid.

3. Summary and future plans

The results indicate that the evolution of the secondary instability that is responsible for the generation of three-dimensionality in the near wake is not captured well in the current simulations. This discrepancy could result from inadequate resolution of the underlying two-dimensional flow and/or spanwise resolution of the three-dimensional structures. The current simulations have the same number of grid points in the spanwise direction as Beaudan & Moin (1994). However, given that the current simulations use only a 2^{nd}-order accurate spatial discretization, more spanwise grid points might be needed to match the resolution power of the 5^{th}-order scheme. Comparison of the modified wavenumber for the schemes suggests that the 2^{nd}-order scheme might need up to twice the number of grid points to match the resolution of the 5^{th}-order scheme.

It is also clear from the present study that the restriction imposed on the streamwise grid stretching factor when using central schemes represents a severe constraint on mesh design for complex geometries. In this respect, the higher-order upwind biased schemes are more flexible since they allow the use of higer stretching factors and increased resolution can be provided selectively at desired locations. However, it is also evident that even these higher order upwind schemes exhibit significant dissipation, and the scales corresponding to the top half of the wavenumber range, which are crucial for determining the subgrid-scale dissipation, are effectively damped out due to the numerical dissipation. The second-order central difference scheme, on the other hand, preserves the energy in the small scales and allows the subgrid-scale dissipation to have a more significant impact on the resolvable flow field.

Doubling the number of grid points on the cylinder surface improves the results only marginally. Therefore, it is unlikely that the disagreement in results is due to lack of resolution on the cylinder surface. In-plane resolution in the near wake region could also be one cause of the discrepancy. In particular, the restriction on the streamwise stretching ratio and the presence of the concave corner at base of the cylinder result in the near wake having poorer streamwise resolution than the simulation of BM. A systematic spanwise resolution study would require doubling the spanwise grid points which would effectively double the computational resources required. In contrast, doubling the streamwise resolution in the near wake can be accomplished with about a 30% increase in computational resources and is thus the more viable next step.

The near-term objective then is to obtain wall and near wake statistics which are independent of the near wake in-plane resolution. 2-D simulations, which are relatively cheap, can be used to give a rough estimate of the in-plane resolution requirement. Once statistics which are independent of the in-plane resolution in the near wake are obtained, these will be compared with the results of BM. If the wall and near wake statistics match reasonably well with BM, this will imply that the spanwise resolution is adequate and the next step will then be to obtain and compare the statistics in the downstream wake region. On the other hand, if the wall and near wake statistics do not match with BM, this will be an indication that increased spanwise resolution might be required. The code is in the process of

being ported to the IBM SP2 parallel computer where the turnaround time will be significantly reduced and it will be possible to use larger meshes.

REFERENCES

BEAUDAN, P. & MOIN, P. 1994 Numerical Experiments on the Flow Past a Circular Cylinders at Sub-Critical Reynolds Numbers. *Report No. TF-62, Thermosciences Div., Dept. of Mech. Engr., Stanford Univ.*

CAIN, A. B. & BUSH, R. H. 1994 Numerical Wave Propagation Analysis for Stretched Grids. *AIAA-paper 94- 0172.*

CHOI, H., MOIN, P. & KIM, J. 1992 Turbulent Drag Reduction: Studies of Feedback Control and Flow Over Riblets. *Report No. TF-55, Thermosciences Div., Dept. of Mech. Engr., Stanford Univ.*

GHOSAL, S., LUND, T. S., MOIN, P. & AKSELVOLL, K. 1995 A Dynamic Localization Model for Large-Eddy Simulation of Turbulent Flows. *J. Fluid Mech.* **286,** 229-255.

GRESHO, P. M. & LEE, R. L. 1981 Don't Suppress the Wiggles-They're Telling You Something!. *Comput. Fluids.* **9,** 223-253.

LOURENCO, L. M. & SHIH, C. 1993 Characteristics of the Plane Turbulent Near Wake of a Circular Cylinder. A Particle Image Velocimetry Study. *Private Communication.*

MITTAL, R. & BALACHANDAR, S. 1995 Effect of Three- Dimensionality on the Lift and Drag of Nominally Two- Dimensional Cylinders. *Phys. Fluids.* **7,** (8), 1841-1865.

MOIN, P., SQUIRES, K., CABOT, W. & LEE, S. 1991 A Dynamic Subgrid-Scale Model for Compressible Turbulence and Scalar Transport. *Phys. Fluids A.* **3,** 2746-2757.

ONG, L., & WALLACE, J. 1994 Private Communication.

RAI, M. M. & MOIN, P. 1993 Direct Numerical Simulation of Transition and Turbulence in a Spatially Evolving Boundary Layer. *J. Comp. Phys.* **109,** No. 2, 169-192.